

# Low density expansion and isospin dependence of nuclear energy functional: comparison between relativistic and Skyrme models

C. Providência,<sup>1</sup> D.P.Menezes,<sup>2</sup> L. Brito,<sup>1</sup> and Ph. Chomaz<sup>3</sup>

<sup>1</sup>*Centro de Física Teórica - Dep. de Física - Universidade de Coimbra - P-3004 - 516 - Coimbra - Portugal*

<sup>2</sup>*Depto de Física - CFM - Universidade Federal de Santa Catarina Florianópolis - SC - CP. 476 - CEP 88.040 - 900 - Brazil*

<sup>3</sup>*GANIL (DSM-CEA/IN2P3-CNRS), B.P. 5027, F-14076 Caen Cédex 5, France*

In the present work we take the non relativistic limit of relativistic models and compare the obtained functionals with the usual Skyrme parametrization. Relativistic models with both constant couplings and with density dependent couplings are considered. While some models present very good results already at the lowest order in the density, models with non-linear terms only reproduce the energy functional if higher order terms are taken into account in the expansion.

PACS number(s): 21.65.+f,24.10.Jv,21.30.-x,21.60.-n

## I. INTRODUCTION

Both non-relativistic and relativistic phenomenological nuclear models are nowadays used to describe successfully nuclear matter and finite nuclei within a density functional formalism. One of the most commonly used non-relativistic models, the Skyrme force model, has been extensively used in the literature since the work of Vautherin and Brink [1]. The Skyrme effective interaction has been improved since its first version [2] in order to account for the different properties of nuclei, not only along the stability line, but also for exotic nuclei from the proton to the neutron drip line and to yield a good description of neutron stars [3]. Along this line, many different versions of the Skyrme effective force have been developed and tested and the importance of the asymmetry discussed [3, 4]. In [5], the results of the variational microscopic calculations, in which many-body and some relativistic corrections were included, were parametrized. In [4] the Skyrme model parameters were chosen so as to fit the EoS given in [5]. In [6] 87 different parametrizations, which give similar results for finite nuclei experimental observables, were checked against neutron star properties and 60 of them were ruled out. Some of the non-relativistic models include also a three-body force [7] in order to solve the causality problem, reproduce saturation properties of nuclear matter and improve the description of the symmetry energy.

Relativistic models, on the other hand, are advantageous if high density matter, such as the one existing in compact stars, is described, and in particular no lack of causality arises as density increases. As seen in [6], neutron star properties depend on the correct choice of the equation of state (EoS) and the same problem appears within relativistic models, which can be parametrized in different ways, all of them giving similar results for finite nuclei and nuclear matter or neutron matter. Once the EoS is extrapolated to high densities, quantities as symmetry energy, for example, depend a lot on the parameter set chosen [8, 9]. At subsaturation densities,

there is an unstable region, which varies a lot and present different behaviors according to the parametrization chosen [10, 11, 12]. Some relativistic models introduce the density dependence through the couplings of baryons to mesons [13, 14, 15] and once again the instability region at low densities and the EoS at high densities are sensible to the model considered [11, 15]. We point out that the saturation mechanism of relativistic and non-relativistic models is different. For the first ones saturation is attained due to the relativistic quenching of the scalar field. On the other hand, non-relativistic models have to introduce three-body repulsive interactions in order to describe saturation correctly.

At very low densities both, the relativistic and the non-relativistic approaches predict a liquid-gas phase transition region for nuclear matter leading, for dense star matter to a non-homogeneous phase commonly named *pasta phase*, formed by a competition between the long-range Coulomb repulsion and the short-range nuclear attraction [16].

In the past some attempts have already been made in order to compare nuclear matter and finite nuclei properties obtained both with relativistic and non-relativistic models [11, 17, 18] but there is no clear or obvious explanations for the differences. In the following we compare the Skyrme effective force with relativistic nuclear mean-field models at subsaturation densities with the goal to directly compare the energy functional. We expect that the same physics should be contained in both approaches at these densities and therefore it maybe fruitful to compare both types of models in this range of densities.

We start with a brief review of the Skyrme parametrizations of the nuclear energy density functional. Next we consider relativistic mean-field models with constant couplings, namely the initially proposed parametrizations including only linear terms for the meson contributions [19] and parametrizations with non-linear terms [20, 21, 22]. Then we extend our investigation to density dependent models [10, 13, 14, 23, 24]. We compare the non-relativistic limit of their binding energies with the binding energy functional obtained with the non-relativistic Skyrme model. Various levels of the approximation are then discussed.

## II. SKYRME FUNCTIONAL

The non relativistic Skyrme energy functional is defined by

$$B_{\text{Skyrme}} = \mathcal{K} + \mathcal{H}_0 + \mathcal{H}_3 + \mathcal{H}_{\text{eff}},$$

where  $\mathcal{K}$  is the kinetic-energy density,  $\mathcal{H}_0$  a density-independent two-body term,  $\mathcal{H}_3$  a density-dependent term, and  $\mathcal{H}_{\text{eff}}$  a momentum-dependent term:

$$\mathcal{K} = \frac{\tau}{2M}, \quad (1)$$

$$\mathcal{H}_0 = C_0\rho^2 + D_0\rho_3^2, \quad (2)$$

$$\mathcal{H}_3 = C_3\rho^{\sigma+2} + D_3\rho^\sigma\rho_3^2, \quad (3)$$

$$\mathcal{H}_{\text{eff}} = C_{\text{eff}}\rho\tau + D_{\text{eff}}\rho_3\tau_3, \quad (4)$$

where  $\rho = \rho_p + \rho_n$  is the total baryonic density,  $\rho_p$  and  $\rho_n$  being the proton and the neutron densities respectively,  $\rho_3 = \rho_p - \rho_n$ , the isovector density,  $\tau = \sum_{i=p,n} \tau_i$ , the total kinetic density,  $\tau_i = k_{F_i}^5/5\pi^2$  being the kinetic density of each type of particles  $i$  with a Fermi momentum  $k_{F_i}$ , and  $\tau_3 = \tau_p - \tau_n$  the isovector kinetic term. We introduce the following quantities:  $B_1$  the symmetric matter potential energy,  $B_3$  the potential part of the symmetry energy and  $M_i^*$  the proton ( $i = p$ ) or neutron ( $i = n$ ) effective masses,

$$B_1(\rho) = C_0\rho^2 + C_3\rho^{\sigma+2}, \quad (5)$$

$$B_3(\rho) = D_0 + D_3\rho^\sigma, \quad (6)$$

$$M_i^{*-1} = M^{-1} + 2C_{\text{eff}}\rho + \tau_{3i} 2D_{\text{eff}}\rho_3, \quad (7)$$

such that

$$B_{\text{Skyrme}} = \sum_{i=p,n} \frac{\tau_i}{2M_i^*} + B_1(\rho) + \rho_3^2 B_3(\rho). \quad (8)$$

The coefficients  $C_i$  and  $D_i$ , associated respectively with the symmetry and asymmetry contributions, are linear combinations of the traditional Skyrme parameters :

$$\begin{aligned} C_0 &= 3t_0/8 \\ D_0 &= -t_0(2x_0 + 1)/8 \\ C_3 &= t_3/16 \\ D_3 &= -t_3(2x_3 + 1)/48 \\ C_{\text{eff}} &= [3t_1 + t_2(4x_2 + 5)]/16 \\ D_{\text{eff}} &= [t_2(2x_2 + 1) - t_1(2x_1 + 1)]/16 \end{aligned}$$

and  $\sigma$  parametrizes the density dependent term. The  $\sigma$  exponent has a direct effect on the incompressibility. A decrease in  $\sigma$  generates a lower value for the incompressibility [3]. Using  $\rho_i = k_{F_i}^3/3\pi^2$  the kinetic terms can be directly related to the respective density

$$\tau_i = a(\rho_i)^{5/3}$$

where we have introduced  $a = 3^{5/3}\pi^{4/3}/5$ . Looking at small asymmetries  $\rho_p = (\rho \pm \rho_3)/2$  we get

$$\tau = a \left( \rho^{5/3} + \frac{5}{9} \rho^{-1/3} \rho_3^2 \right) \quad (9)$$

$$\tau_3 = \frac{5a}{3} \rho^{2/3} \rho_3 \quad (10)$$

Then it is easy to decompose the kinetic energy density  $\mathcal{K}_{\text{eff}} = \mathcal{K} + \mathcal{H}_{\text{eff}}$  into a symmetric matter component and a symmetry kinetic energy

$$\mathcal{K}_{\text{eff}} = \mathcal{K}_{\text{eff}_1} + \rho_3^2 \mathcal{K}_{\text{eff}_3}$$

leading to

$$\mathcal{K}_{\text{eff}_1} = a\rho^{5/3} \left( \frac{1}{2M} + C_{\text{eff}}\rho \right)$$

$$\mathcal{K}_{\text{eff}_3} = a\frac{5}{9}\rho^{-1/3} \left[ \frac{1}{2M} + (C_{\text{eff}} + 3D_{\text{eff}})\rho \right]$$

The isoscalar part of the effective mass  $C_{\text{eff}}$  directly contributes to  $\mathcal{K}_{\text{eff}_1}$  but also contributes to the symmetry energy because of the asymmetry in the Fermi energy. Indeed as in the Fermi gas model the two first terms of  $\mathcal{K}_{\text{eff}_3}$  can be recasted as  $\mathcal{K}_{\text{eff}_3} = 5\mathcal{K}_{\text{eff}_1}/9\rho^2$ . The last term is an additional term coming from the isovector part of the effective mass. These various contributions to the kinetic energy play an important role both in the binding energy and saturation properties of symmetric matter and in the isospin dependence usually discussed in terms of symmetry energy. When comparing with relativistic approaches the discussion of the kinetic part becomes even more important since the role played by the effective mass and interaction are known to be in general rather different. In Table I we present the nuclear matter saturation properties obtained with the Skyrme forces used in the present work. We consider a conventional Skyrme interaction SIII, one of the recent Skyrme-Lyon interactions designed to describe neutron-rich matter SLy230a [3], the NRAPR parametrization which stands for the Skyrme interaction parameters obtained from a fitting to the EoS of a microscopic model [4, 5] and the LNS parametrization which refers to a recently Skyrme-like parametrization proposed in the framework of the Brueckner-Hartree-Fock approximation for nuclear matter [25].

## III. RELATIVISTIC APPROACHES

### A. The lagrangian

In this section we consider four mean-field relativistic models, which we denote by QHD-II [19], NL3 [20], TM1 [21] and NL $\delta$  [22], with constant coupling parameters described by the Lagrangian density of the linear and non-linear Walecka models (NLWM), with the possible inclusion of the  $\delta$  mesons, given by:

$$\mathcal{L}_{NLWM} = \sum_{i=p,n} \mathcal{L}_i + \mathcal{L}_\sigma + \mathcal{L}_\omega + \mathcal{L}_\rho + \mathcal{L}_\delta, \quad (11)$$

where the nucleon Lagrangian reads

$$\mathcal{L}_i = \bar{\psi}_i [\gamma_\mu iD^\mu - \mathcal{M}^*] \psi_i, \quad (12)$$

with

$$iD^\mu = i\partial^\mu - g_v V^\mu - \frac{g_\rho}{2} \vec{\tau} \cdot \vec{b}^\mu, \quad (13)$$

$$\mathcal{M}^* = M - g_s \phi - g_\delta \vec{\tau} \cdot \vec{\delta}. \quad (14)$$

The isoscalar part is associated with the scalar sigma ( $\sigma$ ) field,  $\phi$ , and the vector omega ( $\omega$ ) field,  $V_\mu$ , while the isospin dependence comes from the isovector-scalar delta ( $\delta$ ) field,  $\delta^i$ , and the isovector-vector rho ( $\rho$ ) field,  $b_\mu^i$  (where  $\mu$  is the 4 dimensional space-time indices and  $i$  the 3D isospin direction indices). The associated Lagrangians are

$$\begin{aligned} \mathcal{L}_\sigma &= +\frac{1}{2} (\partial_\mu \phi \partial^\mu \phi - m_s^2 \phi^2) - \frac{1}{3!} \kappa \phi^3 - \frac{1}{4!} \lambda \phi^4, \\ \mathcal{L}_\omega &= -\frac{1}{4} \Omega_{\mu\nu} \Omega^{\mu\nu} + \frac{1}{2} m_v^2 V_\mu V^\mu + \frac{1}{4!} \xi g_v^4 (V_\mu V^\mu)^2, \\ \mathcal{L}_\delta &= +\frac{1}{2} (\partial_\mu \vec{\delta} \partial^\mu \vec{\delta} - m_\delta^2 \vec{\delta}^2), \\ \mathcal{L}_\rho &= -\frac{1}{4} \vec{B}_{\mu\nu} \cdot \vec{B}^{\mu\nu} + \frac{1}{2} m_\rho^2 \vec{b}_\mu \cdot \vec{b}^\mu, \end{aligned}$$

where  $\Omega_{\mu\nu} = \partial_\mu V_\nu - \partial_\nu V_\mu$ ,  $\vec{B}_{\mu\nu} = \partial_\mu \vec{b}_\nu - \partial_\nu \vec{b}_\mu - g_\rho (\vec{b}_\mu \times \vec{b}_\nu)$ , and  $g_j$  and  $m_j$  are respectively the coupling constants of the mesons  $j = s, v, \rho, \delta$  with the nucleons and their masses. Self-interacting terms for the  $\sigma$ -meson are also included in the three parametrizations,  $\kappa$  and  $\lambda$  denoting the corresponding coupling constants. The  $\omega$ -meson self-interacting term, with the  $\xi$  coupling constant, is present in the TM1 parametrization. In the above Lagrangian density  $\vec{\tau}$  is the isospin operator. The terms involving the  $\delta$  meson are only present in the NL- $\delta$  model and non-linear terms are not present in the simplest version of the model QHD-II. In Table II we present the nuclear matter saturation properties obtained with the relativistic models used in the present work.

## B. Equilibrium

At equilibrium the fermion distribution is a Fermi-Dirac distribution function for nucleons (+) and antinucleons (-)

$$f_{i\pm} = 1 / \{1 + \exp((\epsilon_i^*(\mathbf{p}) \mp \nu_i) / T)\}, \quad (15)$$

where  $\epsilon_i^* = \sqrt{\mathbf{p}^2 + M_i^{*2}}$  with the effective mass

$$M_i^* = M - g_s \phi - \tau_{3i} g_\delta \delta_3, \quad (16)$$

In the equilibrium, the effective chemical potentials are defined by

$$\nu_i = \mu_i - g_v V_0 - \frac{g_\rho}{2} \tau_{3i} b_0, \quad (17)$$

where  $\tau_{3i} = \pm 1$  is the isospin projection for the protons and neutrons respectively. At zero temperature the distribution function reduces to a simple step function

$$f_i = \theta(p_{F_i}^2 - p^2), \quad (18)$$

with

$$p_{F_i} = \sqrt{\nu_i^2 - M_i^{*2}}. \quad (19)$$

Let us introduce  $\phi_0$ ,  $V_0$ ,  $\delta_3$  and  $b_0$  the values of the scalar ( $\sigma$ ), the vector ( $\omega$ ), isovector scalar ( $\delta$ ) and the isovector vector ( $\rho$ ) fields, obtained from the meson equations of motion, considered as static and uniform classical fields

$$m_s^2 \phi_0 + \frac{1}{2} \kappa \phi_0^2 + \frac{1}{6} \lambda \phi_0^3 = g_s \rho_s, \quad (20)$$

$$m_v^2 V_0 + \frac{1}{6} \xi g_v^4 V_0^3 = g_v \rho, \quad (21)$$

$$m_\delta^2 \delta_3 = g_\delta \rho_{s3}, \quad (22)$$

$$m_\rho^2 b_0 = \frac{g_\rho}{2} \rho_3, \quad (23)$$

where the baryonic and scalar densities read:

$$\rho_i = 2 \int \frac{d^3 \mathbf{p}}{(2\pi)^3} \theta(p_{F_i}^2 - p^2), \quad (24)$$

$$\rho_{s_i} = 2 \int \frac{d^3 \mathbf{p}}{(2\pi)^3} \frac{M_i^*}{\sqrt{p^2 + M_i^{*2}}} \theta(p_{F_i}^2 - p^2), \quad (25)$$

and  $\rho = \rho_p + \rho_n$ ,  $\rho_3 = \rho_p - \rho_n$ ,  $\rho_s = \rho_{sp} + \rho_{sn}$ ,  $\rho_{s3} = \rho_{sp} - \rho_{sn}$ . The above ensemble of equations for the effective mass (16), the fields (20)-(23) and the densities (24)-(25) related to the Fermi momentum (19) defines entirely the state in a self-consistent way. In the sequel we introduce the constants  $c_\rho = g_\rho^2 / 8m_\rho^2$  and  $c_\alpha = g_\alpha^2 / 2m_\alpha^2$ , with  $\alpha = s, v, \delta$ .

The energy density is then given :

$$E = K_p + K_n + E_\sigma + E_\omega + E_\delta + E_\rho, \quad (26)$$

with

$$K_i = 2 \int \frac{d^3 \mathbf{p}}{(2\pi)^3} \sqrt{p^2 + M_i^{*2}} \theta(p_{F_i}^2 - p^2), \quad (27)$$

$$E_\sigma = \frac{m_s^2}{2} \phi_0^2 + \frac{1}{6} \kappa \phi_0^3 + \frac{1}{24} \lambda \phi_0^4, \quad (28)$$

$$E_\omega = \frac{m_v^2}{2} V_0^2 + \frac{1}{8} \xi g_v^4 V_0^4 \quad (29)$$

$$E_\delta = \frac{m_\delta^2}{2} \delta_3^2 = c_\delta \rho_{s3}^2, \quad (30)$$

$$E_\rho = c_\rho \rho_3^2, \quad (31)$$

Having solved the field's self-consistent equations entirely defines the system energy functional.

In order to compare the relativistic approaches with the non relativistic one we also look at the binding energy density defined as

$$B = E - M\rho. \quad (32)$$

Isolating the kinetic contribution

$$T_i = K_i - M_i^* \rho, \quad (33)$$

we can define an interaction part

$$B_{\text{exact}}(\rho, \rho_3) = B - \sum_i T_i, \quad (34)$$

which can be decomposed into an isoscalar part

$$B_{1\text{exact}}(\rho) = B_{\text{exact}}(\rho, \rho_3 = 0) \quad (35)$$

and isovector potential energy contributions

$$B_{3\text{exact}}(\rho, \rho_3) = \frac{B_{\text{exact}}(\rho, \rho_3) - B_{1\text{exact}}(\rho)}{\rho_3^2}. \quad (36)$$

Using these notations the binding energy from relativistic approaches can be recasted as in the Skyrme case

$$B = \sum_i T_i + B_{1\text{exact}}(\rho) + B_{3\text{exact}}(\rho, \rho_3) \rho_3^2. \quad (37)$$

We also separate the effective mass into the isoscalar and the isovector channels and write

$$M_i^* = M + M_1 + \tau_{3i} \rho_3 M_3. \quad (38)$$

#### IV. DIRECT COMPARISON OF ENERGY FUNCTIONAL

The first idea to make a bridge between the classical and relativistic models is to directly compare the various terms entering in the associated energy functionals. Indeed, considering the Kohn-Sham theorem, models leading to the same energy functional are strictly equivalent as far as physical results are concerned. However, in the previous sections, we have seen that for spin saturated static matter the Skyrme energy is a functional of the isoscalar and isovector particle and kinetic densities. The case of the relativistic models is more complex since the proton and neutron baryonic and scalar densities appear as well as the relativistic kinetic energy density. This makes a direct comparison of the functional impossible. In this paper we thus adopt two strategies: i) In the next section we develop a non-relativistic approximation to these densities in order to reduce them to the Skyrme like local densities. Then a direct comparison of the functionals at low densities is possible and will teach us a lot about the connections between those two classes of models. A low density expansion of the energy per particle

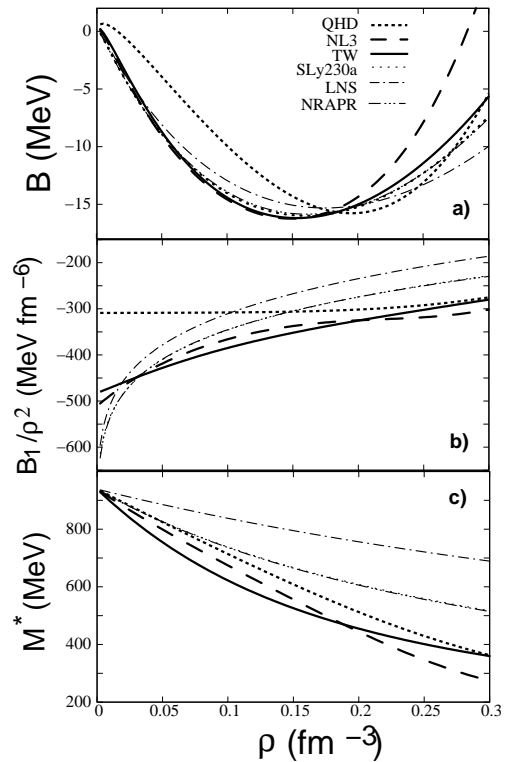


FIG. 1: Symmetric matter: a) Binding energy; b) Isoscalar contribution of the interaction divided by  $\rho^2$ ,  $B_{1\text{exact}}/\rho^2$ ; c) Effective mass for several relativistic and non-relativistic models.

gives

$$\begin{aligned} E/\rho = & M + \frac{3k_F^2}{10M} - \frac{3k_F^4}{56M^3} + \dots + \left( \frac{g_v^2}{2m_v^2} - \frac{g_s^2}{2m_s^2} \right) \rho \\ & + \frac{g_s^2}{m_s^2} \frac{\rho}{M} \left[ \frac{3k_F^2}{10M} - \dots \right] + \left( \frac{g_s^2 \rho}{m_s^2 M} \right)^2 \left[ \frac{3k_F^2}{10M} - \dots \right] \\ & + \mathcal{O} \left[ \left( \frac{g_s^2 \rho}{m_s^2 M} \right)^3 \right]. \end{aligned}$$

where the terms of the type  $\left( \frac{g_s^2 \rho}{m_s^2 M} \right)^n$ ,  $n = 1, 2, 3, \dots$  have origin on the expansion of the scalar density and are equivalent to  $n$ -body terms of the Skyrme interaction generally described by fractionary exponents. ii) Secondly, we look at the contributions of the various energy terms to the nuclear matter EoS thus reducing the functionals of both models to particle densities. With this reduction, exact results for the various models can be directly compared.

Let us first focus on the properties of symmetric matter. In Figs. 1a), 1b) and 1c) we show respectively the binding energy, the isoscalar contribution of the interaction  $B_{1\text{exact}}$  and the effective mass for several relativistic and non-relativistic models. We include the results of the Walecka (QHD-II) model just for comparison although we know it does not reproduce well the properties of nu-

clear matter at saturation. In particular, it has a very high compressibility. A comparison of the binding energies plotted in Fig. 1a) shows that i) although the saturation point is quite close in energy and densities for all models, there is some discrepancy which is related to the way the parametrizations were fitted; ii) relativistic and non-relativistic models show different behaviors above and below saturation density: at subsaturation densities relativistic models show generally more binding (except for the Walecka parametrization) and above saturation density the binding energy decreases faster with density within these models. The parametrization with density dependent coefficients (TW) has a behavior closer to the other non-relativistic models; iii) the second derivatives of the curves are associated with the incompressibility and can be very different. This is just a reflex of the values tabulated for the compressibilities of the different models in Tables I and II.

We next compare the isoscalar term of the interaction. In order to separate the parabolic contribution we represent this term divided by  $\rho^2$ . The Walecka parametrization shows an almost independent behavior on the density because this model has no non-linear terms on the  $\sigma$ -meson. Non-relativistic and relativistic models show similar behaviors although the last ones do not grow so fast with density. This tendency will be compensated by the density dependence of the effective mass in the two types of models. In fact, the effective mass decreases faster in the relativistic models as compared with non-relativistic models, as seen in Fig. 1c). Smaller effective masses give rise to larger kinetic energy contributions so that the kinetic energy contribution to the total energy is more important in relativistic models. We should stress, however that the effective masses in relativistic and non-relativistic models have different meanings. For the first type the effective mass includes the contribution of the nucleon scalar self-energy, while for the second type the effective mass reflects the momentum dependence of the single particle energy. We point out that the isoscalar channel of the Skyrme parametrizations SLy230a and LNS are very similar. These two parametrizations show differences in the isovector channel.

Let us now turn to the isospin dependence. We focus the discussion on the symmetry energy, the exact isovector term of the interaction  $B_3$  [Eq. (36)] and the isospin channel of the effective mass  $M_3$ . We include the relativistic models with non-linear terms on the  $\rho-\omega$  mesons which allow a more flexible description of the isovector channel. From Fig. 2a), one observes that the slopes of the symmetry energy are somewhat different when considering a relativistic or a non-relativistic model, TW being the only relativistic model that shows a behaviour similar to the non-relativistic ones. The other relativistic models show an approximately linear dependence of the symmetry energy on the density. It has recently been discussed in [26] that there is a linear correlation between the neutron skin thickness and the slope of the symmetry energy for non-relativistic models and this fact gives

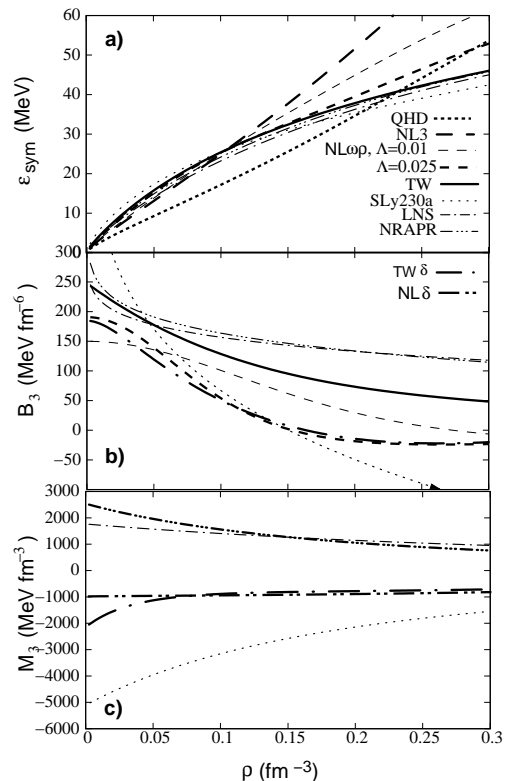


FIG. 2: Isospin channel: a) symmetry energy; b) exact  $B_3$ ; c) isospin channel of effective mass  $M_3$ .

a very strong constraint on the density dependence of the nuclear symmetry energy and consequently on the EoS as well. In [27] it was found that the same kind of correlation exists for density dependent relativistic models.

The isovector channel of the interaction, Fig. 2, also shows a large discrepancy between the different models and also between models within the same framework: in particular the SLy230a shows a behavior very different for the other Skyrme parametrizations, with a very fast decrease with density becoming even negative for  $\rho > 0.15 \text{ fm}^{-3}$ . The relativistic models with the non-linear  $\omega-\rho$  terms or with density dependent couplings including the  $\delta$  meson also become negative at large densities but this effect is not so pronounced.

In relativistic models there is a proton-neutron mass splitting only if the scalar isovector  $\delta$ -meson is included. This occurs for the DDH $\delta$  and NL $\delta$  parametrizations we consider. As we see from Fig 2c),  $M_3 = (M_p^* - M_n^*)/\rho_3$  is negative for these models which corresponds to a  $M_n^* < M_p^*$  in neutron rich nuclear matter. A similar behavior is predicted by the Skyrme interaction SLy230a but an opposite behavior is obtained with the LNS and NRAPR parametrizations of the Skyrme interaction. A discussion of the isospin dependence of the effective mass has been done in [28]. The proton-neutron mass splitting is a present topic of discussion and the forthcoming experiments with radioactive beams will allow the clarification

of this point.

From the figures just discussed we conclude that the isoscalar channel already shows some discrepancy between the different models, mainly between the relativistic and the non-relativistic ones. However the larger discrepancies occur for the isovector channel. In this case there is not even a general common trend between the models of each class.

## V. NON-RELATIVISTIC APPROXIMATION TO THE ENERGY FUNCTIONAL

In what follows we perform a non-relativistic expansion of the energy density [Eq. (26)] in order to make a comparison with a classical approximation like the Skyrme one. This approximation is based on the expansion

$$\epsilon_i^* = \sqrt{\mathbf{p}^2 + M_i^{*2}} \simeq M_i^* + \frac{\mathbf{p}^2}{2M_i^*}. \quad (39)$$

In order to be valid the Fermi momentum should be small compared to the nucleon effective mass meaning that such an expansion is restricted to low densities. Then we have the scalar density and the relativistic kinetic energy written as functionals of the particle and kinetic densities:

$$\rho_{s_i} \simeq \rho_i - \frac{\tau_i}{2M_i^{*2}}, \quad (40)$$

$$K_i \simeq M_i^* \rho_i + \frac{\tau_i}{2M_i^*}. \quad (41)$$

Using these two approximations we have reduced the relativistic densities to the standard densities appearing in the Skyrme approaches. Solving now the field equations it becomes easy to recast the relativistic energy functional in a Skyrme form for the considered case, depending only on particles and kinetic densities. Since this equivalence is obtained at the first order in  $p^2/M^2$  we obtain analytical expressions for the fields at the same level of approximation.

### A. QHD-II

In order to test the non-relativistic approximation of the relativistic models we first consider the QHD-II parametrization [19]. In this case the non-linear terms are zero ( $\kappa = 0$ ,  $\lambda = 0$ , and  $\xi = 0$ ) and the  $\delta$  meson is not present ( $c_\delta = 0$ ).

Then, the  $\omega$  field is directly deduced from Eq. (21)

$$V_0 = g_v \rho / m_v^2, \quad (42)$$

and so is the  $\rho$  field from Eq. (23)

$$b_0 = \frac{g_\rho}{2} \rho_3 / m_\rho^2. \quad (43)$$

In the same spirit, the  $\sigma$  field is directly deduced from Eq. (20) leading to

$$\phi_0 = g_s \rho_s / m_s^2. \quad (44)$$

Using the expansion (40) of the scalar density  $\rho_s$ , the  $\sigma$  field can be explicitly written as a functional of  $\rho$  and  $\tau$

$$g_s \phi_0 = 2c_s \left( \rho - \frac{\tau}{2M^{*2}} \right). \quad (45)$$

Since in this model the  $\sigma$  field is the only contribution to the effective mass, using (16), the effective mass is given by:

$$M^* = M - 2c_s \left( \rho - \frac{\tau}{2M^{*2}} \right). \quad (46)$$

This equation can be solved iteratively replacing  $1/M^{*2}$  on the rhs of equation (46) by  $M^{-2} + 4c_s \rho M^{-3}$ . The different terms of the energy (26) are now all functional of the particle densities and kinetic densities.

$$K_i = \left[ M - 2c_s \left( \rho - \frac{\tau}{2M^{*2}} \right) \right] \rho_i + \frac{\tau_i}{2M^*}, \quad (47)$$

$$E_\sigma = c_s \rho^2 - c_s \frac{\tau}{M^{*2}} \rho, \quad (48)$$

$$E_\omega = c_v \rho^2, \quad (49)$$

$$E_\rho = \frac{m_\rho^2}{2} b_0^2 = c_\rho \rho_3^2, \quad (50)$$

and the energy functional can be analytically compared with the Skyrme one, the differences being both in the functional dependence and in the coefficients. Then grouping the  $K_i$  and  $E_\sigma$  terms helps to recognize the different terms of the Skyrme functional:

$$\sum_i K_i + E_\sigma = \sum_{i=p,n} (M \rho_i + T_i) + E'_\sigma,$$

with

$$T_i = \frac{\tau_i}{2M^*},$$

$$E'_\sigma = -c_s \rho^2,$$

where the effective mass is approximated by Eq. (46).

We can now look at the binding energy density given by Eq.(32) which becomes

$$B_{\text{non-rel.}} = \sum_{i=p,n} T_i + E'_\sigma + E_\omega + E_\rho. \quad (51)$$

In order to test this Skyrme-like approximation, we rewrite the functional  $B_{\text{non-rel.}}$  in the form of Eq. (8) and obtain

$$B_1(\rho) = (c_v - c_s) \rho^2, \quad (52)$$

$$B_3(\rho) = c_\rho. \quad (53)$$

In Figs. 4a) we compare the approximate binding energy,  $B_{\text{non-rel.}}$ , Eq. (51), with its exact value, Eq. (32), the quantities  $B_1(\rho)$ , eq (52) with  $B_{1,\text{exact}}(\rho)$  defined in Eq. (35) and  $M^*$ , Eq. (46) with  $M_{\text{exact}}^* = M - g_s\phi_0$ . In all cases we can see that the non-relativistic approximation is a good approximation for low densities when the Fermi momentum is not too high. Thus, we can safely compare the functional obtained in this limit with the Skyrme one.

We can see that the above non-relativistic limit of this first simple relativistic model (QHD-II) leads to a Skyrme functional as far as the density dependence is concerned (see Eqs. (5) and (6) ), with a simple two body force ( $C_3$  and  $D_3$  are both zero). As already referred, we point out that the three-body term in the Skyrme parametrization is essential to get saturation. For the simple Walecka model the quenching of the scalar field will play a similar role. The effective mass is similar but not identical since the Skyrme parametrization Eq. (7) applies to  $M^{*-1}$  while the relativistic models introduce directly  $M^*$  (see Eq. (46)). Moreover the relativistic models in their non-relativistic limit present a richer parametrization of the effective mass with non linear contributions in the kinetic energy density. However, the leading orders are similar.

It should be noticed that, for this simple model, without a  $\delta$  field the isospin dependence of the effective mass is not introduced. In the next section we study the isospin dependence of the mass.

In order to introduce non-trivial density dependence, we also consider models with interacting fields such as the non-linearities in the  $\sigma$  models or the non-linear  $\sigma\rho$  and  $\omega\rho$  couplings (see section V C). An alternative way is to directly introduce density dependent coupling parameters as discussed in section V D.

### B. $\delta$ and non-linearities in the $\sigma$ and $\omega$ fields

In this section, we cure the two problems encountered in the simple model discussed above introducing the  $\delta$  field in order to produce an isospin dependent mass splitting between protons and neutrons and a non-linear  $\sigma$  and  $\omega$  field to modify the density dependence of the energy functional.

The first step is to solve the field equations. Let us first start with the  $\delta$  field which can be easily solved introducing the approximate scalar field (40) in the field equation (22). We obtain for the  $\delta_3$  field

$$\delta_3 = 2\frac{c_\delta}{g_\delta}(\rho_{s_p} - \rho_{s_n}) = 2\frac{c_\delta}{g_\delta}\rho_3 - \Delta_{K3}, \quad (54)$$

with

$$\Delta_{K3} = \frac{c_\delta}{g_\delta}\left(\frac{\tau_p}{M_p^{*2}} - \frac{\tau_n}{M_n^{*2}}\right).$$

Turning now to the  $\sigma$  field we have to solve the self-consistent problem relating  $\phi_0$  to the proton and neutron scalar fields (20) which can be computed as a function of

the proton and neutron effective masses, Eq. (40), which is a function of the  $\sigma$  field, Eq. (16). In the case of small non-linear terms, the  $\sigma$  field can be perturbatively solved.

Indeed, in a simple and crude approximation, the  $\kappa$  and  $\lambda$  terms are assumed to be small, and then from Eq. (20) the leading term becomes:

$$g_s\bar{\phi}_0 = 2c_s(\rho_{s_p} + \rho_{s_n}) = 2c_s\left(\rho - \frac{\tau_p}{2M_p^{*2}} - \frac{\tau_n}{2M_n^{*2}}\right). \quad (55)$$

This approximation can thus be introduced in the non-linear terms to get  $\phi_0 = \bar{\phi}_0 + d\phi$  with, at the lowest order in the non linear terms,

$$d\phi = -\frac{1}{2}\frac{\kappa}{m_s^2}\bar{\phi}_0^2 - \frac{1}{6}\frac{\lambda}{m_s^2}\bar{\phi}_0^3. \quad (56)$$

This leads to

$$\phi_0 = 2\frac{c_s}{g_s}\rho - \Delta_\sigma - \Delta_{K0},$$

with the non-linear and kinetic contributions

$$\begin{aligned} \Delta_\sigma &= 2\kappa\frac{c_s^2}{m_s^2g_s^2}\rho^2 + \frac{4\lambda}{3}\frac{c_s^3}{m_s^2g_s^3}\rho^3, \\ \Delta_{K0} &= \frac{c_s}{g_s}\left(\frac{\tau_p}{M_p^{*2}} + \frac{\tau_n}{M_n^{*2}}\right). \end{aligned}$$

The same strategy can be used to solve the  $\omega$  field either directly from its relation to the baryonic density (cf. Eq. (21)) or assuming that at low density the non-linearities are small and thus solving Eq. (21) iteratively from the linear solution  $\bar{V}_0 = g_v\rho/m_v^2$ . Then at the first iteration we get

$$V_0 = \frac{g_v\rho}{m_v^2} - \frac{1}{6}\xi g_v^7\frac{\rho^3}{m_v^8}. \quad (57)$$

The expressions for  $\phi_0$  and  $\delta_3$  can now be used to obtain the non-relativistic approximation for the effective mass in the form of Eq. (38), with

$$M_1 = -2c_s\rho + g_s\Delta_\sigma + g_s\Delta_{K0}, \quad (58)$$

$$M_3 = -2c_\delta + g_\delta\Delta_{K3}/\rho_3. \quad (59)$$

This set of coupled equations can be solved directly or iteratively. At the first iteration the  $(M_i^*)^{-2}$  reads

$$(M_i^*)^{-2} = M^{-2} + 4c_s\rho M^{-3} + 4c_\delta\tau_{3i}\rho_3 M^{-3}. \quad (60)$$

Having solved the equations for the fields and for the effective masses in terms of the particle and kinetic density we can now study the energy functional.

In the present case, the different terms of the energy

read

$$K_i = \rho_i (M - 2c_s \rho - \tau_{3i} 2c_\delta \rho_3 + g_s \Delta_\sigma) \quad (61)$$

$$+ g_s \Delta_{K0} + g_\delta \tau_{3i} \Delta_{K3} + \frac{\tau_i}{2M_i^*}, \quad (62)$$

$$E_\sigma = c_s \rho^2 - g_s \rho (\Delta_\sigma + \Delta_{K0}) + \frac{1}{6} \kappa \phi_0^3 + \frac{1}{24} \lambda \phi_0^4, \quad (63)$$

$$E_\omega = c_v \rho^2 + c_{v4} \rho^4, \quad c_{v4} = -\frac{2}{3} \xi c_v^4, \quad (64)$$

$$E_\delta = c_\delta \rho_3^2 - g_\delta \rho_3 \Delta_{K3}, \quad (65)$$

$$E_\rho = c_\rho \rho_3^2. \quad (66)$$

Then grouping the terms  $K_i$ ,  $E_\sigma$  and  $E_\delta$  leads to the following simplification

$$\sum_i K_i + E_\sigma + E_\delta = \sum_{i=p,n} (M \rho_i + T_i) + E'_\sigma + E'_\delta,$$

with

$$\begin{aligned} T_i &= \frac{\tau_i}{2M_i^*}, \\ E'_\sigma &= -c_s \rho^2 + c_{s3} \rho^3 + c_{s4} \rho^4, \\ E'_\delta &= -c_\delta \rho_3^2, \end{aligned}$$

where the effective mass is given by equation (38) with (58) and (59).

The non-linear effects are included in the additional parameters  $c_{s3} = 4\kappa c_s^3 / 3g_s^3 = \kappa g_s^3 / 6m_s^6$  and  $c_{s4} = 2\lambda c_s^4 / 3g_s^4 = \lambda g_s^4 / 24m_s^8$ .

The binding energy density  $B = E - M\rho$ , reads now

$$B_{\text{non-rel.}} = \sum_{i=p,n} T_i + E'_\sigma + E_\omega + E'_\delta + E_\rho, \quad (67)$$

and we get for  $B_1$  and  $B_3$

$$B_1(\rho) = (c_v - c_s) \rho^2 + c_{s3} \rho^3 + (c_{s4} + c_{v4}) \rho^4, \quad (68)$$

$$B_3(\rho) = c_\rho - c_\delta. \quad (69)$$

As in the simplest QHD model, taking advantage of the non-relativistic limit we have expressed the scalar density and the relativistic kinetic energy density as functionals of  $\rho_i$  and  $\tau_i$ . Then the energy also becomes a functional of  $\rho_i$  and  $\tau_i$  of the form of a Skyrme functional. The interaction part presents a very similar structure. In Figs. 4a), b) and c) we show how the approximation works for NL3, TM1 and NL $\delta$ . While for TM1 the present approximation is good, for NL3 and NL $\delta$  we would have to include higher orders in the density expansion to improve the results. The non-linear coupling in the  $\sigma$  and  $\omega$  fields have introduced higher order terms in the potential energy of symmetric matter. However because of the perturbative approach we have taken we are restricted to a polynomial density dependence. To go beyond this limitation, we have also fitted Skyrme parameters on the exact potential energy functional. The results of this fit

is given in Table V and will be discussed later. As far as the isospin dependence is concerned, the absence of non linearities (or couplings) in isovector fields leads to a rather poor isospin dependence since  $B_3$  is constant. The introduction of a coupling of the isoscalar fields with the isovector  $\rho$  field corrects this fact. Finally, the main difference is again in the functionals describing the effective mass but now not only the expansions are made for different quantities, the mass in relativistic approach and the inverse mass in the Skyrme model, but also the relativistic approaches lead to a much richer functional of both  $\rho_i$  and  $\tau_i$ .

### C. Non-linear $\sigma\rho$ and $\omega\rho$ couplings

Still a different model includes non-linear  $\sigma - \rho$  and  $\omega - \rho$  couplings [23, 24] which allow to change the density dependence of the symmetry energy. In the corresponding Lagrangian a new coupling term  $\mathcal{L}_{\sigma\omega\rho}$  is added:

$$\mathcal{L}_{\sigma\omega\rho} = g_\rho^2 \vec{b}_\mu \cdot \vec{b}^\mu [\Lambda_s g_s^2 \phi^2 + \Lambda_v g_v^2 V_\mu V^\mu]. \quad (70)$$

We have followed the prescription of [23] so that the coupling  $\Lambda_i$  is chosen in such a way that for  $k_F = 1.15 \text{ fm}^{-1}$  (not the saturation point) the symmetry energy is 25.68 MeV like in the NL3 parametrization. We start by setting  $\Lambda_s = 0$  as in [30]. In this case, the equations of motion are not the standard ones, once two of them become coupled and, for this reason, they are reproduced as follows:

$$g_v V_0 = \frac{g_v^2}{m_v^2} [\rho - 2g_v V_0 g_\rho^2 b_0^2 \Lambda_v],$$

$$\frac{g_\rho}{2} b_0 = \frac{g_\rho^2}{4m_\rho^2} [\rho_3 - 4g_\rho b_0 g_v^2 V_0^2 \Lambda_v].$$

If the  $\Lambda_s$  is not assumed to be zero but no non-linearity is taken into account either in the  $\sigma$  or in the  $\omega$  field (i.e.  $\kappa = 0$ ,  $\lambda = 0$  and  $\xi = 0$ ), the three fields are coupled in the following way:

$$g_s \phi_0 = \frac{g_s^2}{m_s^2} [\rho_s - 2g_s \phi_0 g_\rho^2 b_0^2 \Lambda_s],$$

$$g_v V_0 = \frac{g_v^2}{m_v^2} [\rho - 2g_v V_0 g_\rho^2 b_0^2 \Lambda_v],$$

$$\frac{g_\rho}{2} b_0 = \frac{g_\rho^2}{4m_\rho^2} [\rho_3 - 4g_\rho b_0 (g_s^2 \phi_0^2 \Lambda_s + g_v^2 V_0^2 \Lambda_v)].$$

This set of equations should be solved self consistently. However, if the  $\Lambda_s$  and  $\Lambda_v$  are small we can solve the problem perturbatively introducing  $\phi_0 = \frac{g_s}{m_s^2} \rho_s$ ,  $V_0 = \frac{g_v}{m_v^2} \rho$  and  $b_0 = \frac{g_\rho}{2m_\rho^2} \rho_3$  in the right hand side of the above

equations

$$\begin{aligned} g_s \phi_0 &= 2c_s \rho_s [1 - 64c_s c_\rho^2 \rho_3^2 \Lambda_s], \\ g_v V_0 &= 2c_v \rho [1 - 64c_v c_\rho^2 \rho_3^2 \Lambda_v], \\ \frac{g_\rho}{2} b_0 &= 2c_\rho \rho_3 [1 - 64c_\rho (c_s^2 \rho_s^2 \Lambda_s + c_v^2 \rho^2 \Lambda_v)]. \end{aligned}$$

then the binding energy reads

$$B = \sum_{i=p,n} T_i + E'_\sigma + E_\omega + E'_\delta + E_\rho + E_{\rho sv}, \quad (71)$$

where the last term is the interaction energy between the  $\rho$  and the  $\sigma$  and  $\omega$  fields

$$E_{\rho sv} = g_\rho^2 b_0^2 [\Lambda_s g_s^2 \phi_0^2 + \Lambda_v g_v^2 V_0^2].$$

In this case,

$$T_i = \frac{\tau_i}{2M_i^*}, \quad (72)$$

$$E'_\sigma = -c_s \rho^2, \quad (73)$$

$$E_\omega = c_v \rho^2 - 2c_{v\rho} \rho^2 \rho_3^2, \quad (74)$$

$$E'_\delta = -c_\delta \rho_3^2, \quad (75)$$

$$E_\rho = c_\rho \rho_3^2 - 2c_{v\rho} \rho^2 \rho_3^2 - 2c_{s\rho} \rho^2 \rho_3^2, \quad (76)$$

$$E_{\rho sv} = c_{s\rho} \rho^2 \rho_3^2 + c_{v\rho} \rho^2 \rho_3^2, \quad (77)$$

with  $c_{v\rho} = 64c_v^2 c_\rho^2 \Lambda_v$ ,  $c_{s\rho} = 64c_s^2 c_\rho^2 \Lambda_s$ . The effective mass can again be approximated by the leading terms of equation (38). It should be noticed that the last term of  $E_{\rho sv}$  partly cancels the  $E_\rho$  correction leading to

$$E_\rho + E_{\rho sv} = c_\rho \rho_3^2 - c_{v\rho} \rho^2 \rho_3^2 - c_{s\rho} \rho^2 \rho_3^2.$$

The  $B$  coefficients are then written as

$$B_1(\rho) = (c_v - c_s) \rho^2 + c_{s_3} \rho^3 + c_{s_4} \rho^4 \quad (78)$$

$$B_3(\rho) = c_\rho - c_\delta - (3c_{v\rho} + c_{s\rho}) \rho^2, \quad (79)$$

where we also include the contributions of the non-linear  $\sigma$  terms. These expressions increase more rapidly with density than the corresponding Skyrme functional contribution given by equations (5-6): for the relativistic model a term with a  $\sigma = 2$  exponent would be necessary while the usual range of the Skyrme parameter  $\sigma$  is below 1 in order to not present a too strong incompressibility. In Fig. 4 we see that the present approximation works well for  $B_1$  and the effective mass  $M^*$  but fails to give a reasonable description of the binding energy. This was expected because NL $\omega\rho$  is just NL3 with non linear  $\omega\rho$  terms. The limitation of the present approximation is also clear for the  $B_3$  term shown in Fig. 6a). Since we are looking at a low density expansion we have also directly fitted Skyrme parameters on the relativistic symmetry energy, Table V.

## D. Density dependent coupling parameters

Next we consider two models with density dependent coupling parameters, respectively the TW model [13] and the DDH $\delta$  [10, 14] which also includes the  $\delta$  meson. These two models do not include self-interaction terms for the meson fields (i.e.  $\kappa = 0$ ,  $\lambda = 0$  and  $\xi = 0$ ). The only difference comes from the replacement of  $g$  coupling constants for the density dependent coupling parameters  $\Gamma_s$ ,  $\Gamma_v$ ,  $\Gamma_\rho$  and  $\Gamma_\delta$  which are adjusted in order to reproduce some of the nuclear matter bulk properties, using the following parametrization for the TW model

$$\Gamma_i(\rho) = \Gamma_i(\rho_{sat}) h_i(x), \quad x = \rho/\rho_{sat}, \quad (80)$$

with

$$h_i(x) = a_i \frac{1 + b_i(x + d_i)^2}{1 + c_i(x + d_i)^2}, \quad i = s, v \quad (81)$$

and

$$h_\rho(x) = \exp[-a_\rho(x - 1)], \quad (82)$$

and  $\Gamma_\delta(\rho) = 0$ , with the values of the parameters  $m_i$ ,  $\Gamma_i$ ,  $a_i$ ,  $b_i$ ,  $c_i$  and  $d_i$ ,  $i = s, v, \rho$  given in [13]. For the DDH $\delta$  model we consider the TW parametrizations of  $\Gamma_s$  and  $\Gamma_v$  and for the other two mesons we take

$$h_i(x) = a_i \exp[-b_i(x - 1)] - c_i(x - d_i), \quad i = \rho, \delta.$$

Such density dependences in the coupling parameters do not affect the expression for the energy functional but of course affect its derivative such as the pressure or the chemical potentials. The latter ones are given by

$$\mu_i = \nu_i + \Gamma_v V_0 + \tau_{i3} \frac{\Gamma_\rho}{2} b_0 + \Sigma_0^R, \quad (83)$$

where the rearrangement term is

$$\Sigma_0^R = \frac{\partial \Gamma_v}{\partial \rho} \rho V_0 + \frac{\partial \Gamma_\rho}{\partial \rho} \rho_3 \frac{b_0}{2} - \frac{\partial \Gamma_s}{\partial \rho} \rho_s \phi_0 - \frac{\partial \Gamma_\delta}{\partial \rho} \rho_{s3} \delta_3.$$

As already discussed in the literature [10, 11, 15], the rearrangement term is crucial in obtaining different behaviors in many quantities related to the chemical potentials or to their derivatives with respect to the density as compared with the more common NL3 or TM1 parametrizations.

The binding energy functional is given by equation (67) with

$$B_1(\rho) = (C_v - C_s) \rho^2 = C_0 \rho^2, \quad (84)$$

$$B_3(\rho) = C_\rho - C_\delta = D_0, \quad (85)$$

$$\begin{aligned} M_i^* &= M - 2C_{s\rho} - \tau_{3i} 2C_\delta \rho_3, \\ &= M - 2C_{\text{eff}\rho} - \tau_{3i} 2D_{\text{eff}} \rho_3, \end{aligned} \quad (86)$$

where the  $C_i$  coefficients are computed replacing the coupling constants  $g_i$  by  $\Gamma_i(\rho)$ .

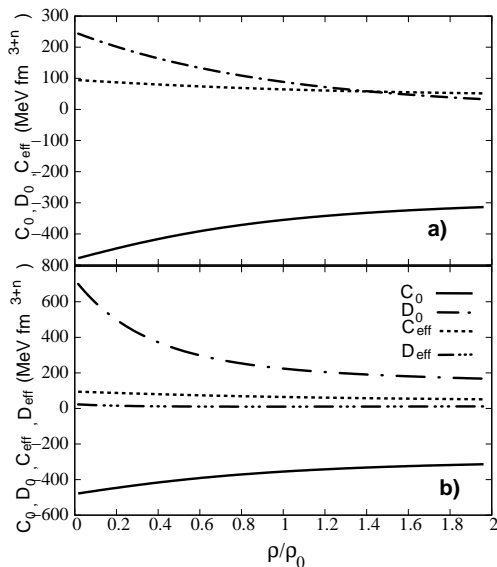


FIG. 3: Coefficients  $C_i$  and  $D_i$  for (a) the TW model and (b) the DDH $\delta$  model.

In Figs. 5 we show the binding energy, the coefficient  $B_1(\rho)$  and the effective mass obtained in the non-relativistic approximation and the corresponding exact values. We see that the low density non-relativistic approximation works quite well both with and without the  $\delta$  meson. The same is true for the  $B_3$  contribution. In Fig. 6b) the exact and approximate coefficients  $B_3(\rho)$  are plotted for these density dependent models (TW and DDH $\delta$ ).

### E. Comparison between relativistic and Skyrme functionals

We now compare the non-relativistic functional obtained from the relativistic models described so far with the Skyrme functional.

In Table III we have collected the terms  $B_1$ ,  $B_3$ ,  $M_1$  and  $M_3$  for the models we have considered in the present work. We notice that for the Skyrme forces the inverse of the effective mass is parametrized according to (7) while for the relativistic models we take a similar expression for the effective mass, Eq. (38). This fact explains the minus sign difference between the two types of models for the  $M_1$  and  $M_3$  columns. Except for the Walecka model, all models have for the isoscalar interaction contribution a parabolic term plus a higher order term on the density. This second contribution appears explicitly through  $\rho^3$  and  $\rho^4$  terms, or implicitly through the density dependence of the coupling parameters for TW and DDH $\delta$ . The isovector interaction contribution has a much poorer parametrization in the relativistic models:  $B_3$  is generally constant because  $D_3 = 0$ , except for the NL $\omega\rho$  model and again the TW and DDH $\delta$  models due to the density

dependence of the coupling parameters.

In Table IV we show the values of these coefficients for the models that we have discussed. One can see that  $C_0$  and  $C_{\text{eff}}$  are of the same order of the corresponding parameters of some Skyrme models shown in [3, 29]. The  $C_3$  coefficients are normally twice as large for relativistic than for non-relativistic models and the  $D_0$  coefficients for relativistic models are half of the coefficients of the non-relativistic ones. An immediate conclusion already referred is the poor parametrization of the isovector channel in the relativistic models: for most models both  $D_3$  and  $D_{\text{eff}}$  are zero. Some comments with respect to the isoscalar channel are also in order: for the relativistic models the scalar kinetic contribution, defined by  $C_{\text{eff}}$  is higher. This is due to the smaller effective mass within these models. The saturation is possible with an overall larger binding for the isoscalar channel. This channel has an attractive term from the two-body force and a repulsive three-body ( $n$ -body) contribution. A larger binding may be obtained with a stronger two-body attractive potential ( $C_0$ ) or a weaker three-body contribution ( $C_3$  together with the  $\sigma$  exponent).

The coefficients of the density dependent models discussed before could not be included in the above table since they are not fixed quantities. In Figs. 3 the coefficients for these models, defined in equations (84-86), are plotted. Their values agree with the ones already given in Table IV for density values  $\rho/\rho_0 > 0.2$ .

In order to better compare the relativistic models, and in particular the parametrizations with density dependent coupling parameters, with several Skyrme force models we have also fitted the exact  $B_1$  and  $B_3$  by the (5) and (6) expressions in the density range  $0 - 0.1 \text{ fm}^{-3}$  using, whenever appropriate, the same value for  $\sigma$  in both expressions. In Table V we give the results of these fits.

Some conclusions can be drawn from the values in Tables IV and V. First of all we conclude that the isoscalar channel in relativistic mean field models has a quite complicated density dependence, both the interaction and momentum dependent term. In Table IV we only give the coefficients of the first terms of the expansion, which, as discussed before, works quite well at low subsaturation densities for QHD-II and TM1 but not so well for NL3, NL $\delta$  and NL $\omega\rho$ . Using expressions (5) and (6) to parametrize the isoscalar and isovector interaction term we have obtained for all the relativistic models a non-integer coefficient  $\sigma$  smaller than 1 except for the QHD-II. This is a special case which, as we know, does not describe correctly nuclear matter properties, namely, it predicts a very large compressibility. All other  $\sigma$  values are smaller than 1 but not so small as the corresponding parameter in Skyrme forces with good performances which are generally below 0.2. This small value of  $\sigma$  in Skyrme forces controls the compressibility and is generally taken equal to 1/6. Another term which has a very systematic behavior is the isoscalar momentum dependent term described by  $C_{\text{eff}}$ : this coefficient, except for the NL $\delta$ , is larger than 50 and maybe as large as  $\sim 100$

MeV fm<sup>5</sup> for the TW. This occurs at low densities and is compensated by an extra binding coming from the attractive term described by  $C_0$ . Non-relativistic models have a similar behaviour, i.e.,  $C_{\text{eff}} \sim 50 \text{ MeV fm}^5$ . It should be noticed however that TW has a richer density dependence which is parametrized by the coefficient  $C_{\text{eff},3}$  not present in the Skyrme forces. On the other hand, relativistic models have generally a very simple isovector channel. The inclusion of the  $\delta$ -meson brings in the extra degree of freedom missing in the momentum dependent terms but not in the interaction term if only linear terms are included for the mesons. Models with density dependent coefficients such as the TW include automatically a larger density dependence in the isovector term of the interaction. When we compare  $D_3$  for TW with  $D_3$  for SLy230a, NRAPR or LNS we observe a similar behavior.

## VI. CONCLUSIONS

In the present work, we have compared relativistic mean-field nuclear models the relativistic models with the non-relativistic Skyrme models. We have shown that for the isoscalar channel the relativistic models behave in a similar way, and generally different from the non-relativistic description. This is true for the binding energy, isoscalar interaction term and effective mass. The relativistic density dependent models give the closer description to the one obtained by the non-relativistic models.

The isovector channel has proved to be a different problem: there is a quite big discrepancy even between models

within the same framework. This is the least known part of the nuclear interaction which we expect to determine with the future radioactive beams. Relativistic models have generally a very poor description of the this channel.

We have next tried to obtain a low density expansion of the relativistic models with a parametrization similar to the one used for the Skyrme interactions. The energy functional of the relativistic models depends not only on the isoscalar and isovector particle and kinetic densities but also on the isoscalar and isovector scalar densities. Only in the low density regime these densities reduce to the respective particle densities. We have shown that for some models already in the subsaturation density expansions it is necessary to include many terms in order to get good agreement. For the low density range for which there is a good agreement between the low density expansion and the exact values, we have shown that some of the coefficients of the relativistic and the non-relativistic models are of the same order of magnitude. However we have shown that for the first ones the scalar kinetic contribution is higher. The saturation is possible with an overall larger binding for the isoscalar channel which is due to a stronger two-body attractive potential or a weaker three-body contribution.

## ACKNOWLEDGMENTS

This work was partially supported by CNPq (Brazil), CAPES(Brazil)/GRICES (Portugal) under project 100/03 and FEDER/FCT (Portugal) under the projects POCTI/FP/63419/2005 and POCTI/FP/63918/2005.

- 
- [1] D. Vautherin and D.M. Brink, Phys. Rev. **C 3**, 626 (1972).
  - [2] T. H. R. Skyrme, Phil. Mag. **1**, 1043 (1956); Nucl. Phys. **abf 9**, 615 (1959).
  - [3] E. Chabanat, P. Bonche, P. Haensel, J. Meyer and R. Schaeffer, Nucl. Phys. **A 627**, 710 (1997); M. Beiner, H. Flocard, N. van Giai and P. Quentin, Nucl. Phys. **A 238**, 29 (1975).
  - [4] A.W. Steiner, M. Prakash, J.M. Lattimer and P.J. Ellis, Phys. Rep. **411** 325 (2005).
  - [5] A. Akmal, V.R. Pandharipande and D.G. Ravenhall, Phys. Rev. **58**, 1804 (1998).
  - [6] J.R. Stone, J.C. Miller, R. Koncewicz, P.D. Stevenson, M. R. Strayer, Phys. Rev. **68**, 034324 (2003).
  - [7] R.B. Wiringa, V. Fiks and A. Fabrocini, Phys. Rev. **C 38** 1010 (1988); W. Zuo, A. Lejeune, U. Lombardo and J. F. Mathiot, Nucl. Phys. **A 706**, 4180 (2002); W. Zuo, A. Lejeune, U. Lombardo and J. F. Mathiot, Eur. Phys. J. **A 14**, 469 (2002).
  - [8] A.M.S. Santos and D.P. Menezes, Phys. Rev. **C 69**, 045803 (2004).
  - [9] D.P. Menezes and C. Providência, Phys. Rev. **C 68**, 035804 (2003); Braz. J. Phys. **34**, 724 (2004).
  - [10] S.S. Avancini, L. Brito, D. P. Menezes and C. Providência, Phys. Rev. **C 70**, 015203 (2004).
  - [11] S.S. Avancini, L. Brito, Ph. Chomaz, D.P. Menezes and C. Providência, Phys. Rev. **C 74**, 024317 (2006).
  - [12] C. Providência, L. Brito, S.S. Avancini, D. P. Menezes and Ph. Chomaz, Phys. Rev. **C 73**, 025805 (2006).
  - [13] S. Typel and H. H. Wolter, Nucl. Phys. **A 656**, 331 (1999).
  - [14] T. Gaitanos, M. Di Toro, S. Typel, V. Baran, C. Fuchs, V. Greco and H. H. Wolter, Nucl. Phys. **A 732**, 24 (2004).
  - [15] S.S. Avancini and D.P. Menezes, Phys. Rev. **C 74**, 015201 (2006).
  - [16] D. G. Ravenhall, C. J. Pethick, and J. R. Wilson, Phys. Rev. Lett. **50**, 2066 (1983); M. Hashimoto, H. Seki, and M. Yamada, Prog. Theor. Phys. **71**, 320 (1984).
  - [17] B.A. Li, C.M. Ko and W. Bauer, Inter. J. Mod. Phys. **E 7**, 147 (1998).
  - [18] K. Pomorski, P. Ring, G.A. Lalazissis, A. Baran, Z. Lojewski, B. Nerlo-Pomorska, M. Warda, Nucl. Phys. **A 624**, 349 (1997).
  - [19] B.D. Serot and J.D. Walecka, Adv. Nucl. Phys. **16**, 1 (1986).
  - [20] G. A. Lalazissis, J. König and P. Ring, Phys. Rev. **C 55**, 540 (1997).

- [21] K. Sumiyoshi, H. Kuwabara, H. Toki, Nucl. Phys. **A 581**, 725 (1995).
- [22] B. Liu, V. Greco, V. Baran, M. Colonna and M. Di Toro, Phys. Rev. C **65**, 045201 (2002).
- [23] C.J. Horowitz and J. Piekarewicz, Phys. Rev. Lett. **86**, 5647 (2001).
- [24] J.K. Bunta and S. Gmuca, Phys. Rev. C **68**, 054318 (2003).
- [25] L. G. Cao, U. Lombardo, C. W. Shen and N. Van Giai, Phys. Rev. C **73**, 014313 (2006).
- [26] L. Chen, C.M. Ko and B. Li, nucl-th/0610057.
- [27] S.S. Avancini, J.R. Marinelli, D.P. Menezes, M.M.W. Moraes and C. Providência, Phys. Rev. C (2007), in press, nucl-th/0704.0407.
- [28] V. Baran, M. Colonna, V. Greco and M. di Toro, Phys. Rep. 410,335 (2005).
- [29] F. Douchin, P. Haensel, J. Meyer, Nucl. Phys. **A 665**, 419 (2000)
- [30] J.K. Bunta and S. Gmuca, Phys. Rev. C **70**, 054309 (2004).

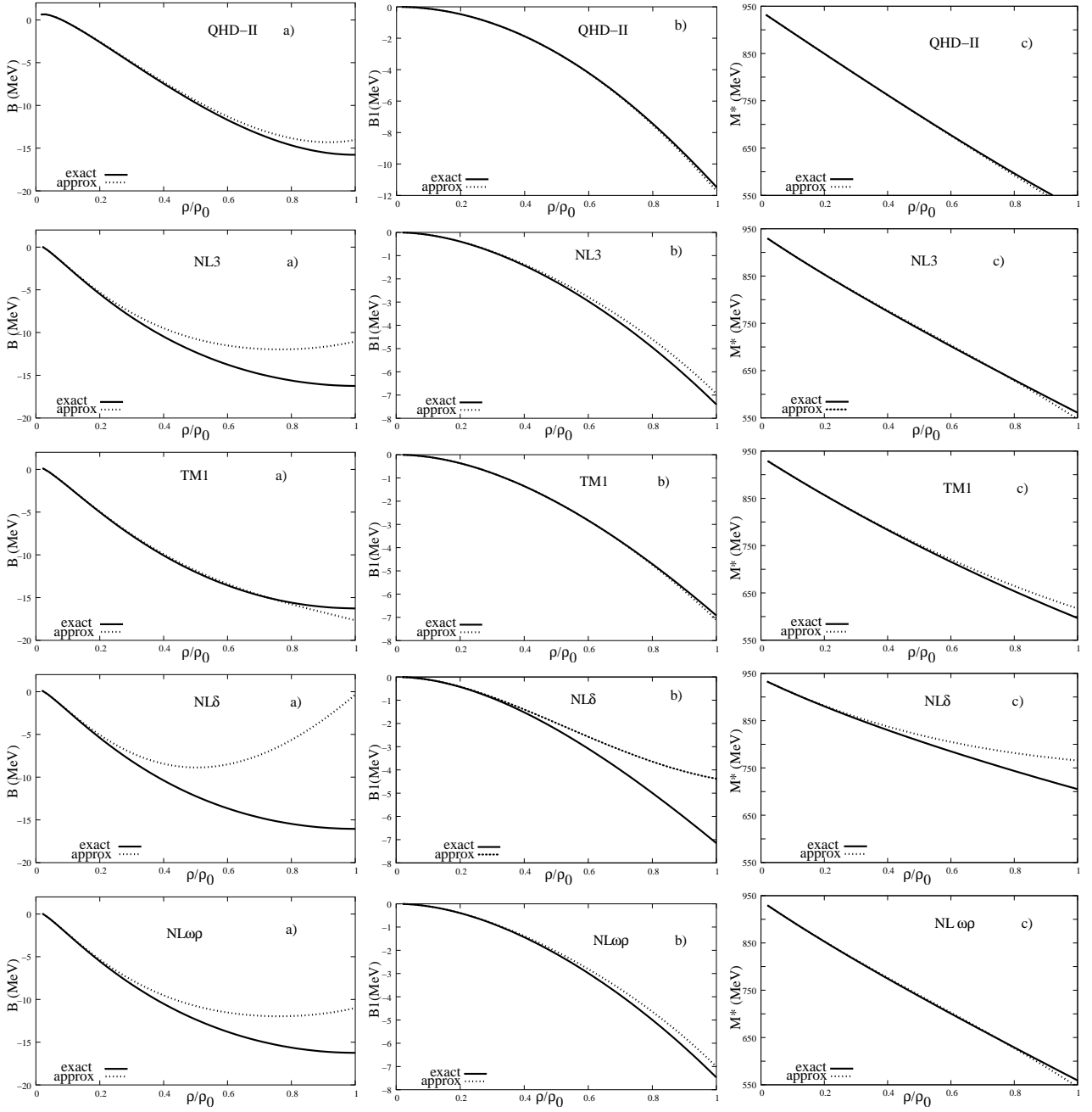


FIG. 4: Comparison between several exact and approximate physical quantities: a) binding energy density, b)  $B_1(\rho)$  coefficient and c) effective mass  $M^*$  for relativistic models with constant couplings.

Model	$B/A$ (MeV)	$\rho_0$ (fm <sup>-3</sup> )	$K$ (MeV)	$\mathcal{E}_{sym}$ (MeV)	$M^*/M$
SIII [3]	15.851	0.145	355.5	28.16	0.76
SLy230a [3]	15.989	0.16	229.87	31.97	0.697
NRAPR [4]	15.86	0.16	225.7	32.79	0.7
LNS [25]	15.32	0.175	210.85	33.4	0.825

TABLE I: Nuclear matter properties of the Skyrme forces used in the present work

Model	$B/A$ (MeV)	$\rho_0$ (fm <sup>-3</sup> )	$K$ (MeV)	$\mathcal{E}_{sym}$ (MeV)	$M^*/M$
Walecka [19]	15.75	0.192	540	22.1	0.556
NL3 [20]	16.3	0.148	272	37.4	0.60
TM1 [21]	16.3	0.145	281	36.9	0.63
NL $\delta$ [22]	16.0	0.160	240	30.5	0.60
TW [13]	16.3	0.153	240	32.0	0.56
DDH $\delta$ [14]	16.3	0.153	240	25.1	0.56

TABLE II: Nuclear matter properties of the relativistic models used in the present work

TABLE III: Expressions for the coefficients  $B_1(\rho)$ ,  $B_3(\rho)$ ,  $M_1(\rho)$  and  $M_3(\rho)$ . For the Skyrme parametrization we take (7) which refers to  $M^{*-1}$ .

model	$B_1(\rho)$	$B_3(\rho)$	$M_1(\rho)/\rho$	$M_3(\rho)$
Skyrme	$C_0\rho^2 + C_3\rho^{\sigma+2}$	$D_0 + D_3\rho^\sigma$	$2C_{\text{eff}}$	$2D_{\text{eff}}$
QHD-II	$(c_v - c_s)\rho^2$	$c_\rho$	$-2c_s$	
NL3, TM1	$(c_v - c_s)\rho^2 + c_{s3}\rho^3 + (c_{s4} + c_{v4})\rho^4$	$c_\rho$	$-2c_s$	
NL $\delta$	$(c_v - c_s)\rho^2 + c_{s3}\rho^3 + (c_{s4} + c_{v4})\rho^4$	$c_\rho - c_\delta$	$-2c_s$	$-2c_\delta$
NL $\omega\rho$ , NL $\sigma\omega$	$(c_v - c_s)\rho^2 + c_{s3}\rho^3 + c_{s4}\rho^4$	$c_\rho - (3c_{v\rho} + c_{s\rho})\rho^2$	$-2c_s$	
TW	$(C_v - C_s)\rho^2$	$C_\rho$	$-2C_s$	
DDH $\delta$	$(C_v - C_s)\rho^2$	$C_\rho - C_\delta$	$-2C_s$	$-2C_\delta$

TABLE IV: Coefficients  $C_i$  and  $D_i$  obtained in the present work and results from several Skyrme models.

model	$C_0$ (MeV fm <sup>3</sup> )	$C_3$ (MeV fm <sup>3+3σ</sup> )	$D_0$ (MeV fm <sup>3</sup> )	$D_3$ (MeV fm <sup>3+3σ</sup> )	$C_{\text{eff}}$ (MeV fm <sup>5</sup> )	$D_{\text{eff}}$ (MeV fm <sup>5</sup> )	$\sigma$
QHD-II	-308.83	0	59.30	0	50.97	0	1
NL3	-511.34	2482.69	131.44	0	68.01	0	1
NL $\omega\rho, \Lambda_v = 0.01$	-511.34	2482.69	149.22	-5975.74 ( $\sigma = 2$ )	68.01	0	1
NL $\omega\rho, \Lambda_v = 0.025$	-511.34	2482.69	189.76	-24161.25 ( $\sigma = 2$ )	68.01	0	1
TM1	-479.21	1571.51	138.34	0	64.90	0	1
NL $\delta$	-482.07	2369.38	63.82	0	44.64	10.81	1
SIII [3]	-426.28	875	268.08	0	44.38	-30.63	1
Sk1' [29]	-396.49	903.97	208.42	0	12.98	-20.99	1
SLy230a [3]	-933.84	862.69	1015.89	-1392.89	56.37	56.37	1/6
NRAPR [4]	-1019.89	940.13	449.80	-398.68	57.015	-27.992	0.14416
LNS [25]	-931.86	911.76	349.62	-283.17	25.05	-19.5	1/6

TABLE V: Coefficients obtained from the fitting to the exact  $B_1$  and  $B_3$  expressions

model	$C_0$ (MeV fm <sup>3</sup> )	$C_3$ (MeV fm <sup>3+3σ</sup> )	$D_0$ (MeV fm <sup>3</sup> )	$D_3$ (MeV fm <sup>3+3σ</sup> )	$C_{\text{eff},0}$ (MeV fm <sup>5</sup> )	$C_{\text{eff},3}$ (MeV fm <sup>3+3σ</sup> )	$D_{\text{eff}}$ (MeV fm <sup>5</sup> )	$\sigma$
QHD-II	-297.0	253.625	59.30	0	50.97	0	0	2.5
NL3	-625.25	546.28	131.44	0	68.01	0	0	0.318
TM1	-482.84	546.07	138.34	0	64.90	0	0	0.606
NL $\delta$	-594.83	802.09	63.82	0	44.64	0	10.81	0.536
TW	-486.09	613.50	251.92	-746.72	96.29	-136.80	0	0.767

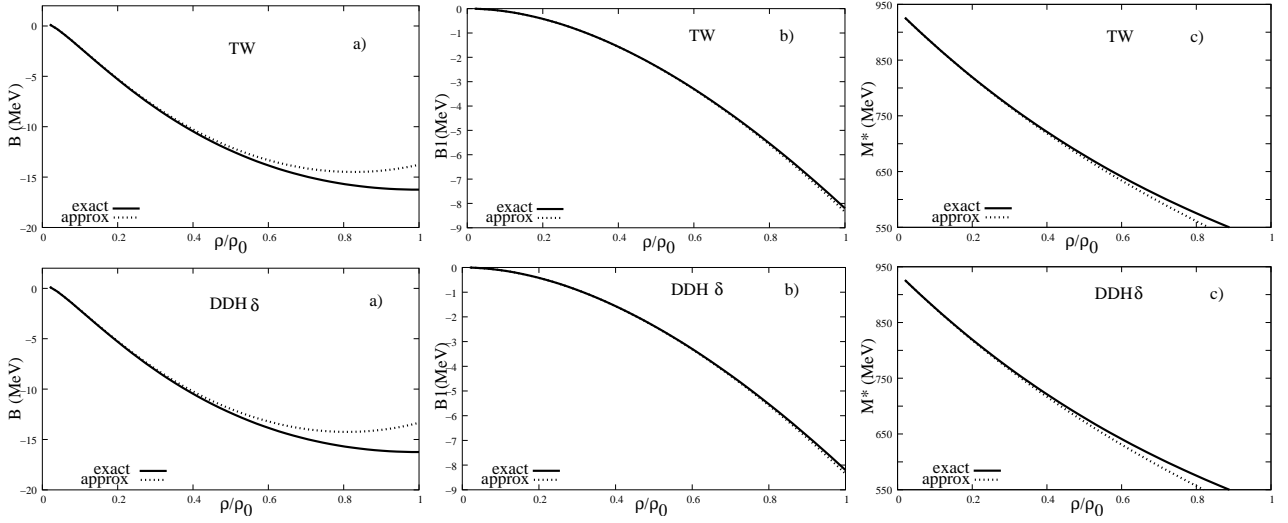


FIG. 5: Comparison between several exact and approximate physical quantities: a) binding energy density, b)  $B_1(\rho)$  coefficient and c) effective mass  $M^*$  for relativistic models with density dependent couplings.

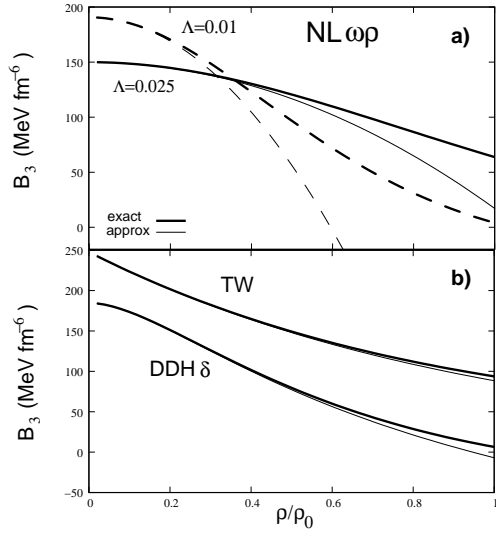


FIG. 6:  $B_3(\rho)$  coefficient for a) a non-linear coupling model ( $NL\omega\rho$ ) and b) two density dependent models TW and  $DDH\delta$ .